RESEARCH ARTICLE | *Immunometabolic Cross-Talk and Regulation of Endocrine and Metabolic Functions*

Aging impairs mouse skeletal muscle macrophage polarization and muscle-specific abundance during recovery from disuse

Paul T. Reidy,[1] Alec I. McKenzie,[1] Ziad S. Mahmassani,[1] Jonathan J. Petrocelli,[1] Daniel B. Nelson,[2]
Catherine C. Lindsay,[3] James E. Gardner,[3] Vincent R. Morrow,[1] Alexandra C. Keefe,[4]
Thomas B. Huffaker,[5] Greg J. Stoddard,[6] Gabrielle Kardon,[4] Ryan M. O'Connell,[5] and
Micah J. Drummond[1,2,5]

[1]*Department of Physical Therapy and Athletic Training, University of Utah, Salt Lake City, Utah;* [2]*Department of Nutrition
and Integrative Physiology, University of Utah, Salt Lake City, Utah;* [3]*School of Medicine, University of Utah, Salt Lake City,
Utah;* [4]*Human Genetics, University of Utah, Salt Lake City, Utah;* [5]*Department of Pathology, University of Utah, Salt Lake
City, Utah; and* [6]*Division of Epidemiology, University of Utah, School of Medicine, Salt Lake City, Utah*

Reidy PT, McKenzie AI, Mahmassani ZS, Petrocelli JJ, Nelson DB, Lindsay CC, Gardner JE, Morrow VR, Keefe AC, Huffaker TB, Stoddard GJ, Kardon G, O'Connell RM, Drummond MJ. Aging impairs mouse skeletal muscle macrophage polarization and muscle-specific abundance during recovery from disuse. *Am J Physiol Endocrinol Metab* 317: E85–E98, 2019. First published April 9, 2019; doi:10.1152/ajpendo.00422.2018.—Impaired recovery of aged muscle following a disuse event is an unresolved issue facing the older adult population. Although investigations in young animals have suggested that rapid regrowth of skeletal muscle following a disuse event entails a coordinated involvement of skeletal muscle macrophages, this phenomenon has not yet been thoroughly tested as an explanation for impaired muscle recovery in aging. To examine this hypothesis, young (4–5 mo) and old (24–26 mo) male mice were examined as controls following 2 wk of hindlimb unloading (HU) and following 4 (RL4) and 7 (RL7) days of reloading after HU. Muscles were harvested to assess muscle weight, myofiber-specifc cross-sectional area, and skeletal muscle macrophages via immunofluorescence. Flow cytometry was used on gastrocnemius and soleus muscle (at RL4) single-cell suspensions to immunophenotype skeletal muscle macrophages. Our data demonstrated impaired muscle regrowth in aged compared with young mice following disuse, which was characterized by divergent muscle macrophage polarization patterns and muscle-specifc macrophage abundance. During reloading, young mice exhibited the classical increase in M1-like (MHC II$^+$CD206$^-$) macrophages that preceeded the increase in percentage of M2-like macrophages (MHC II$^-$CD206$^+$); however, old mice did not demonstrate this pattern. Also, at RL4, the soleus demonstrated reduced macrophage abundance with aging. Together, these data suggest that dysregulated macrophage phenotype patterns in aged muscle during recovery from disuse may be related to impaired muscle growth. Further investigation is needed to determine whether the dysregulated macrophage response in the old during regrowth from disuse is related to a reduced ability to recruit or activate specific immune cells.

hindlimb suspension; immune; regrowth; supporting cells

INTRODUCTION

It is well documented that aging in rodents and humans is accompanied by impaired muscle regrowth/recovery following disuse atrophy (2, 25, 44, 45, 53, 55). This may be a contributing factor in the development of sarcopenia with aging (53). Unfortunately, there is a large gap in knowledge of the cellular and molecular events that govern regrowth in aged muscle following disuse. This knowledge will be an important step to develop appropriate mechanistic-based interventions to offset these deficits in muscle function with aging.

In young muscle, regrowth after disuse elicits a complex yet synchronous process involving many cell types. In particular, macrophages, immune cells of the myeloid lineage, play an important role during muscle regeneration following toxin-induced injury (1) and regrowth following disuse (12, 14, 49). Although skeletal muscle has "resident" immune cells following injury, or other stimuli, circulating immune cells are recruited to the muscle via the vasculature by unique chemotactic signals to assist in promoting repair (10). Early studies in young animals using pharmacological or genetic approaches (12, 14, 15, 49) have demonstrated the requirement of macrophages during the recovery process from disuse.

Macrophages exist under a spectrum of polarized states but in general can be characterized as either pro (M1-like)- or anti-inflammatory (M2-like). During muscle recovery following disuse in young rats, skeletal muscle macrophages initiate an early peak (2–5 days) in M1-like macrophages to clear out debris and prompt muscle satellite cell proliferation (9, 46). This is followed by a shift toward a peak (5–10 days) in M2-like macrophages, which release growth factors (i.e., IGF-I) to promote fibrogenesis, angiogenesis, and satellite cell differentiation, thereby restoring muscle size and function (9, 46). The timing of key recovery events, including satellite cell function, is impaired during muscle regeneration following toxin-induced injury in aging muscle (3, 7). However, the role of macrophages during muscle regrowth in aged animals following disuse is unknown.

Previous reports studying regrowth from disuse in rodents have used immunohistochemistry to characterize macrophage

timing and expression patterns (12, 18, 19, 43, 46–49). Unfortunately, immunohistochemistry has limited quantitative application and potential for nonspecificity of the macrophage marker antigens. For example, macrophage markers commonly utilized in immunohistochemistry may nonspecifically bind to neutrophils, dendritic cells, satellite cells, or other cell types (37, 48). Therefore, we have used a novel application of flow cytometry of mononuclear cells of skeletal muscle in this model of disuse/regrowth to specifically identify and quantify muscle macrophages through a precise and specific myeloid gating strategy.

The purpose of these experiments were to test and characterize the early time course of skeletal muscle macrophage polarization following recovery from disuse in old versus young male mice. We hypothesized that dysregulated skeletal muscle macrophage responses (M1-like and M2-like) during recovery from disuse corresponding to impaired muscle recovery observed in aging muscle.

MATERIALS AND METHODS

Animals. Male C57BL/6 young (4–5 mo) and old (24–26 mo) mice (Jackson Laboratories and National Institutes of Health/National Institute on Aging) were used in this study. We chose to use mice (rather than rats) in order for us to translate our data to the future use of genetic knockout mice as we begin to investigate more specific/mechanistic questions. Animals were housed with ad libitum access to food and water and maintained on a 12:12-h light-dark cycle. All experimental procedures were conducted in accordance with the guidelines set by The University of Utah Institutional Animal Care and Use Committee.

Hindlimb unloading and reloading. A schema of the design can be found in Supplemental Fig. 1A. Mice were divided into four experimental groups: ambulatory controls (CON), 2 wk of hindlimb unloading (HU), HU followed by 4 days of reloading (RL4), and HU followed by 7 days of reloading (RL7). Approximately 6–7 young and 7–11 old mice were assessed at CON and HU time points, whereas ~11–14 young and old mice per group were assessed during reloading (RL4 and RL7). Animals assigned to CON were able to freely ambulate in their cage (2–3 animals/cage) and had ad libitum access to food (standard chow) and water during the experimental periods. For the HU and RL groups, animals underwent hindlimb suspension (2 animals/cage) using a modified unloading method based on the traditional Morey-Holton design for studying disuse atrophy in rodents (17), with additional modifications (26). Body weight and food intake were monitored every other day to ensure that mice were not experiencing excessive weight loss due to malnutrition or dehydration. Following *day 14* of HU, HU animals were fasted for 5 h and then euthanized for tissue analysis (below), while the RL animals were removed from the suspension apparatus and then housed in individual cages for 4 or 7 days of ambulatory recovery (RL4 or RL7, respectively). We chose the 4- and 7-day reloading time points because previous data in young mice indicated that the M1-like macrophage response peaked 3–5 days following reloading and that the M2-like macrophage response followed soon thereafter (7–10 days) (48). On *day 14* of HU or at the respective reloading time points, mice were fasted for 5 h and then euthanized under isoflurane. Triceps, plantaris, and soleus muscles and the lateral head of the gastrocnemius were rapidly dissected, weighed, frozen in liquid nitrogen or OCT (Fisher) in isopentane, and stored at −80°C for later analysis. In the case of flow cytometry analysis, the remaining gastrocnemius muscle (from left and right legs) was dissected and immediately processed for flow cytometry. Whole body tissue com-
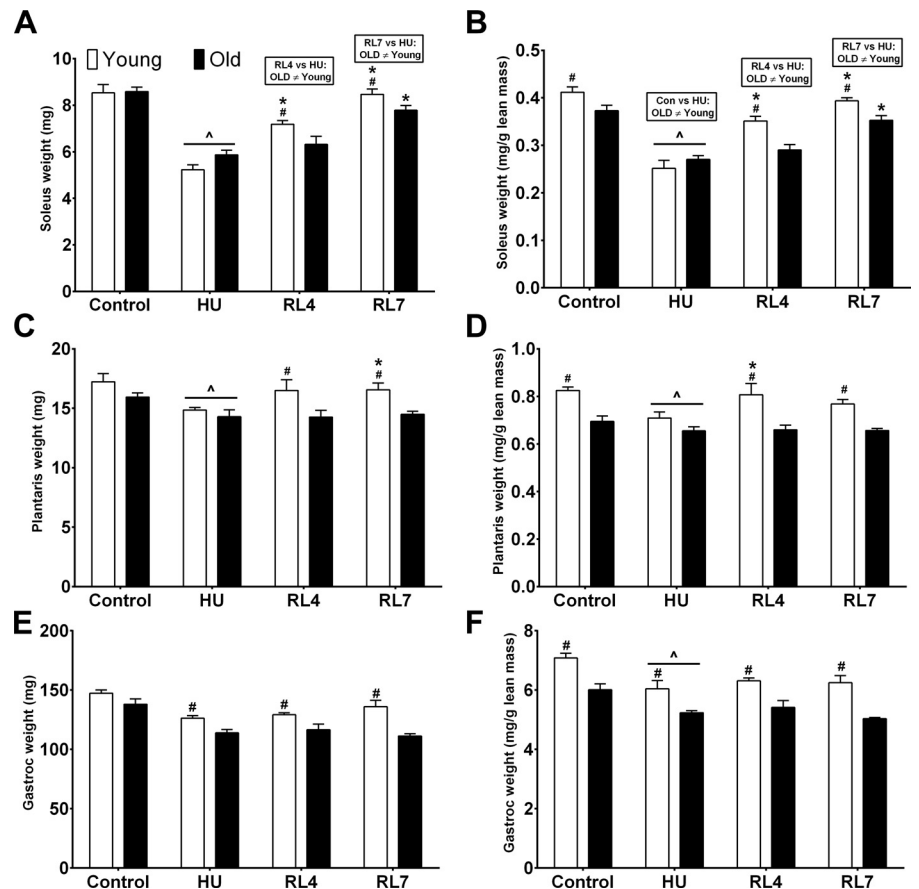

Fig. 1. Soleus, plantaris, and gastrocnemius muscle weights in OLD and YOUNG mice from ambulatory controls and during hindlimb unloading (HU) and reloading (RL). RL4, 4 days of RL; RL7, 7 days of RL. Soleus (*A*), plantaris (*C*), and gastrocnemius (*E*) absolute weights. Soleus (*B*), plantaris (*D*), and gastrocnemius (*F*) weights relative to total body lean mass. #$P < 0.05$ vs. Old; *$P < 0.05$ vs. HU; ^$P < 0.05$ vs. Control.

position was assayed with a Minispec MQ20 NMR analyzer (Bruker, Rheinstetten, Germany).

Flow cytometry and fluorescence-assisted cell sorting. For flow cytometric analysis, muscle cells were isolated with liberase digestion as previously described (33). Cell viability was confirmed using DAPI. Prior to staining, cells were blocked in filtered 1% BSA-PBS, pH 7.4, with addition of Fc-block (cat. no. 14-0161-82, eBioscience). Cell preparations were stained with anti-CD45-Percp.Cy7 (cat. no. 103114, Biolegend), anti-CD11b-PerCpCy5.5 (cat. no. 101228, Biolegend), anti-Ly6c-FITC (cat. no. 128006, Biolegend) anti-F480-PE (cat. no. 123110, Biolegend), anti-CD206-APC (cat. no. 141708, Biolegend), and anti-MHC II-BV510 (cat. no. 107635, Biolegend) antibodies. Immunophenotyping was conducted with a 5-laser (UV,405,488,561,640) BD FACSAria with Diva software v. 6.1.3 (BD Biosciences San Jose, CA). Data were analyzed using FlowJo software. Compensation was conducted manually with single-color controls in gastrocnemius single-cell suspensions. Gating strategy (Fig. 4A) was determined as outlined below, and specificity was determined with fluorescence minus one control staining. After gating out debris, we excluded doublets and selected live (DAPI$^-$)CD45$^+$CD11b$^+$ cells as our myeloid monocyte/macrophage population of interest. Representative quantification of gating strategy was as follows, with letters in parentheses denoting populations of interest (Fig. 4B). Live (DAPI$^-$)CD45$^+$CD11b$^+$ populations of interest (C, K). M1-like macrophages (F4/80$^+$) as MHC II$^+$CD206$^-$ cells (C). M2-like macrophages (F4/80$^+$) as MHC II$^-$CD206$^+$ cells (D). Ratio of M2-like to M1-like macrophages (F4/80$^+$) (E). Ly6c was used to indentify inflammatory monocytes/macrophages divided into the following populations: Ly6c^{High}F4/80^{High} cells (F), Ly6c^{Low}F4/80^{High} cells (G), Ly6c^{Medium}F4/80^{Low} cells (H), Ly6c^{Low}F4/80^{Medium} cells (I), Ly6c$^+$F4/80$^-$ cells (J), and Ly6c$^-$F4/80$^+$ cells (K).

Additionally, we conducted fluorescence-assisted cell sorting (FACS) at the RL4 time point, with both the soleus and gastrocnemius muscles using a similar gating strategy as described above, with the exception that F4/80 replaced CD64, which has been recently validated in murine skeletal muscle as a resident macrophage marker (50). We sorted live CD45$^+$CD11b$^+$ cells with the above-mentioned BD FACSAria into lysis buffer for downstream RNA isolation with the RNeasy Mini Kit (QIAGEN, Germantown, MD) per the manufacturer's instructions.

Immunofluorescence. Frozen OCT-embedded hindlimb muscle samples (soleus, plantaris, gastrocnemius) were sectioned on a cryostat (Microtome Plus). Stained slides were observed with a fully automated wide-field light microscope (Nikon, Tokyo, Japan) with the ×10 or ×20 objective lens. Images were taken using a highsensitivity Andor Clara CCD camera (Belfast, UK).

Myofiber type was assessed with overnight incubation of sections with BA.D5 (1:75; Developmental Studies Hybridoma Bank, Univ. of Iowa) in 1:1 PBS:supernatant of SC.71 (Developmental Studies Hybridoma Bank, Univ. of Iowa) to visualize myosin heavy chain I (MHC I) and myosin heavy chain IIa (MHC IIa) when incubated in Alexa Fluor 647 (cat. no. A21242, 1:250; Invitrogen, Carlsbad, CA) and Alexa Fluor 488 (cat. no. A21121, 1:500; Invitrogen), respectively. Additionally, incubation with WGA, Alexa Fluor 555 (1:50; Invitrogen, WGA Sampler Kit) was applied to designate myofiber borders for assessment of myofiber-type specific cross-sectional area (CSA). Negative stained fibers were considered to be myosin heavy chain IIb and IIx (MHC IIb+IIx). Myofiber CSA was measured using semiautomatic muscle analysis with segmentation of histology, a MATLAB application (SMASH) (41) alongside ImageJ software. For manual macrophage identification, two stains were utilized on soleus and gastrocnemius sections. Sections were blocked in M.O.M. (Vector, Burlingame, CA) and 2.5% NHS (Vector), counterstained with anti-mouse dystrophin antibody (1:100; Santa Cruz Biotechnology, Dallas, TX) and then with either anti-rat CD68 antibody (1:100; Bio-Rad, Hercules, CA) and anti-rabbit CD163 (1:100, Bio-Rad) or

anti-rat CD206 antibody (1:100, Bio-Rad) and anti-rabbit CD163 (1:100, Bio-Rad). Anti-rat secondary antibody (1:250, AF555, Invitrogen), anti-mouse secondary antibody (1: 500, A488, Invitrogen) and anti-rabbit secondary antibody (1:500, AF647, Invitrogen) were applied and then mounted in DAPI-containing mounting medium (Vector). The CD206 and CD163 costain was conducted only on sections from the RL7 time point, because that is the typical period when M2-like macrophages are thought to be most active.

Muscle-specific macrophage content. The observed differences in macrophage abundance as identified by immunofluorescence (via CD68) between the soleus and gastrocnemius muscles prompted us to validate these differences with flow cytometry in control gastrocnemius, plantaris, and soleus muscles. To accommodate anticipated low immune cell yield from the soleus and plantaris, 30 mice were euthanized, and solei from 10 mice were pooled and plantari from 10 mice were pooled, and this was repeated three times to generate $n = 3$ for each muscle analysis. The same analysis was conducted that was noted above for the gastrocnemius, with emphasis on muscle abundance of CD45$^+$CD11b$^+$F4/80$^+$ cells.

mRNA expression. Procedures are described elsewhere (38). Total RNA was isolated by homogenizing 10–15 mg of tissue with a hand-held homogenizer in lysis solution from the RNeasy Mini Kit (QIAGEN). The RNA was extracted according to the manufacturer's instructions, and concentration was determined using the EPOCH (Take3, BioTek) spectrophotometer. All isolated RNA and cDNA samples were stored at −80°C until analysis. Real-time PCR was carried out with a CFX Connect real-time PCR cycler (Bio-Rad) under similar protocol conditions as reported previously (13, 31) using SYBR Green custom-designed primers. The primer pairs are indicated in the Supplemental information (All supplemental materials are available at https://doi.org/10.6084/m9.figshare.8006354.v1). Cycle threshold (C_T) values of target genes were normalized to the geometric mean of 36B4 and PPARγ, and then fold change values were calculated ($\Delta\Delta C_T$) using YOUNG HU as the reference group. For sorted CD11b cells, 36B4 and RPL13a were used as reference genes, and fold change values were calculated ($\Delta\Delta C_T$) using YOUNG or YOUNG RL4 as the comparator group.

Statistical analysis. All data are shown as means ± SE and were checked for major violations of normality. The primary goal was to test whether old mice recover worse than young mice following disuse atrophy (hindlimb unloading). The recovery periods were 4 days (RL4) and 7 days (RL7) of reambulation following hindlimb immobilization. To achieve this goal, we defined "recovery" as the "change", or difference in means, between HU (14 days of hindlimb unloading) and RL4 and RL7 or RL4 and RL7 pooled, respectively for both old and young mice. A secondary goal was to test the effect of HU by age. To test the effect of age on overall recovery we combined the experimental groups of RL4 and RL7 within each age group and then used a two-way ANOVA, with the factors group and age. This was followed by a priori contrasts (mean comparisons) of interest using Wald posttests. The comparisons were primarily between old and young. To test the effect of age at a specific time of recovery we did the following. To examine the effect of age at 4 days of RL (recovery) we used a t-test to examine differences in the means of RL4 between the OLD and YOUNG groups. To examine the effect of age at 7 days of RL (recovery) we used a t-test to examine differences in the means of RL7 between the OLD and YOUNG groups. To test the recovery within each age group at a specific time of recovery, we did the following. To examine the 4-day recovery, the mean of RL4 was compared with the mean of HU, within each age group, with a t-test. To examine the 7-day recovery, the mean of RL7 was compared with the mean of HU, within each age group, with a t-test.

To examine changes in body weight across the experimental periods, we used mixed-effects linear regression, with one between-groups factor and one repeated-measures factor. Significance was set as $P \leq 0.05$, and trends were noted as $0.05 < P < 0.10$. Analyses

were conducted and graphs were created in GraphPad Prism 7.01 or STATA 14.2 (College Station, TX).

RESULTS

Body weight, tissue composition, and food intake. Body weight between groups [at the end of each animal experiment (data not shown)] was greater in the OLD than in the YOUNG. Body weight was less with HU (vs. control) but not different from RL. When examining the time course of changes in body weight with each mouse (Supplemental Fig. S1) during HU and RL, the OLD were heavier than the YOUNG at all time points. Both groups lost weight during HU (Supplemental Fig. S1), but the weight loss was greater in the OLD than in the YOUNG at *days 6–14* of HU. Finally, the OLD demonstrated weight gain on *day 7* of RL compared with HU, whereas the YOUNG showed weight gain on *days 3–7* of RL compared with HU (Supplemental Fig. S1).

With regard to body composition, OLD mice had greater absolute lean mass and water content than the YOUNG mice across the different experimental conditions (Supplemental Table S1). The OLD mice decreased lean mass and water content after HU. OLD mice had more fat mass at control and following HU compared with YOUNG and less fat mass after HU compared with control. OLD mice also had less fat mass at RL4 compared with HU, whereas YOUNG mice demonstrated greater fat mass at RL7 compared with HU.

Muscle weights. Muscle weights were expressed as absolute weight in grams and relative to lean mass (mg muscle/g lean mass) and are shown in Fig. 1 and Table 1. The soleus and plantaris absolute muscle weights were less following HU (vs. control) for both groups. Following RL, the soleus for the OLD was less than for the YOUNG at RL4 and RL7, but both YOUNG and OLD had greater muscle mass at RL7 (vs. HU), whereas only the YOUNG had a greater mass at RL4 (vs. HU). Therefore, there was an age effect for the difference from HU to RL4 and from HU to RL7. When normalized to lean mass, an identical pattern was observed; however, the soleus in the OLD control was less than in the YOUNG, and the OLD displayed a greater difference between control and HU than the YOUNG. An age effect was observed at RL4 and RL7 such that the OLD had smaller plantari than the YOUNG. Following RL, the plantaris muscle from the OLD was similar to HU, whereas the YOUNG had increased muscle size at RL4 (vs. HU) when normalized to lean mass and RL7 (absolute weights). When normalized to lean mass, the OLD had smaller plantari and gastrocnemius at control than the YOUNG. The gastrocnemius muscle (absolute and normalized to lean mass)

decreased in size following HU independently of age. The OLD gastrocnemius mass was similar after RL (vs. HU), whereas the YOUNG was nonsignifanctly increased at RL7 ($P = 0.063$). The OLD had smaller gastrocnemius mass at HU and during RL than the YOUNG. The triceps muscle was unaffected by HU and was not affected by RL in YOUNG mice; however, OLD mice demonstrated a reduced mass at RL4 (vs. HU), and OLD mice had smaller masses during RL than the YOUNG. When the triceps were expressed relative to lean mass, no differences were evident following HU or RL, but larger values were seen in the YOUNG vs. the OLD.

Myofiber MHC composition. Muscle-specific MHC composition demonstrated minor changes (data not reported). The YOUNG solei contained a lower precentage of MHC I myofibers, and the solei decreased MHC IIa precentage while increasing the MHC IIb+IIx percentage at RL7. The plantari MHC composition was unchanged in the OLD, but in the YOUNG there was increased MHC IIa percentage, decreased MHC IIb+IIx percentage at RL7. MHC IIa percentage increased at RL7 in the gastrocnemius in both age groups.

Myofiber diameter and CSA. Soleus, plantaris, and gastrocnemius mean fiber diameter (MFD) and MHC I, MHC IIa, and MHC IIb+IIx myofiber CSA are shown in Fig. 2. Soleus MFD and soleus MHC I, IIa, and MHC IIb+IIx myofiber CSA decreased following HU (vs. control) and was similar following RL (vs. HU) with no age differences across conditions. Soleus MHC IIa CSA was increased at RL7 (vs. HU) for both groups. Plantaris MFD and plantaris MHC IIa and MHC IIb+IIx myofiber CSA decreased following HU and were increased at RL7 compared with HU. Gastrocnemius MFD and MHC IIa and MHC IIb+IIx myofiber CSA decreased in both groups following HU compared with control. However, at RL7, the OLD CSA was similar to HU, whereas the YOUNG CSA increased compared with HU such that an age effect at RL7 and in the difference from HU to RL7 was evident. Gastrocnemius MHC I myofibers were rare and CSA were similar with control and HU, yet smaller MHC I myofibers were found in the OLD compared with the YOUNG at RL7.

Soleus and gastrocnemius muscle macrophages via immunofluorescence. Quantification of CD68, CD163, and CD206 immunoreactivity on mononuclear cells in soleus and gastrocnemius cross-sections is shown in Fig. 3. Macrophages were severalfold more abundant in the soleus than in the gastrocnemius cross-sections (Fig. 3). CD68$^+$CD163$^-$DAPI$^+$ cells in soleus cross-sections (Fig. 3A) were similar following HU compared with control, but a greater density was seen in the YOUNG at RL7 vs. HU. At RL7, the YOUNG observed a

Table 1. *Muscle weights as both absolute and relative to lean mass at CON, HU, RL4, and RL7*

	Absolute				Relative to Lean Mass			
	Con	HU	RL4	RL7	Con	HU	RL4	RL7
Triceps surae								
Old	158.9 ± 5.8	134.1 ± 3.3†	137.2 ± 5.4	133.6 ± 2.1	6.51 ± 0.60	6.16 ± 0.07	6.37 ± 0.25	6.04 ± 0.04
Young	173.0 ± 3.5#	146.3 ± 2.3#†	152.9 ± 2#	159.5 ± 5.2#	8.32 ± 0.15#	7.00 ± 0.31#	7.47 ± 0.12#	7.41 ± 0.23#
Triceps								
Old	102.1 ± 4.9	102.5 ± 2.5	93.9 ± 3.0*	101.3 ± 2.0	4.46 ± 0.18	4.73 ± 0.15	4.36 ± 0.15	4.59 ± 0.10
Young	107.6 ± 2.9	107.6 ± 1.8	104.3 ± 2.5#	108.2 ± 2.5	5.17 ± 0.12#	5.14 ± 0.18#	5.10 ± 0.18#	5.03 ± 0.11#

Data are means ± SE. Triceps surae is the sum of the soleus, plantaris, and gastrocnemius. Con, Control; Gastroc, gastrocnemius; HU, hindlimb unloading; RL4, 4 days of reloading; RL7, 7 days of reloading. †$P < 0.05$ Control vs. HU; #$P < 0.05$ vs. OLD; *$P < 0.05$ vs. HU.
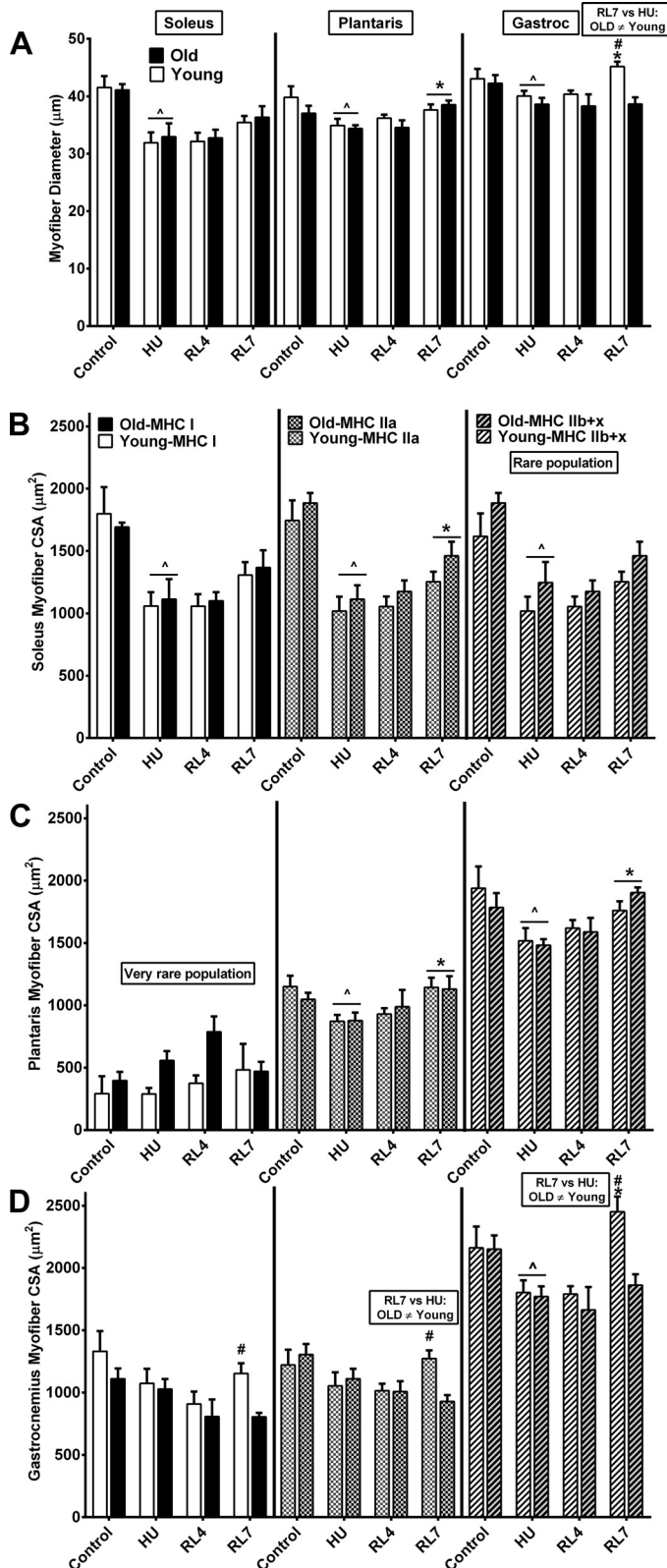
Fig. 2. Soleus, plantaris, and gastrocnemius myofiber size in OLD and YOUNG mice from ambulatory controls and during hindlimb unloading (HU) and reloading (RL). RL4, 4 days of RL; RL7, 7 days of RL. *A*: soleus, plantaris, and gastrocnemius myofiber diameters. Soleus (*B*), plantaris (*C*), and gastrocnemius (*D*) myofiber cross-sectional area by myosin heavy chain (MHC I, IIa, and IIb+IIx) fiber type. #$P < 0.05$ vs. Old; *$P < 0.05$ vs. HU; ^$P < 0.05$ vs. Control.

greater density of $CD68^+CD163^-DAPI^+$ cells vs. HU such that there was a pronounced age effect at RL7 and in the difference from HU to RL7. $CD68^-CD163^+DAPI^+$ cells in soleus cross-sections (Fig. 3*B*) were similar to across conditions and by age. $CD68^+DAPI^+$ cells in soleus cross-sections (Fig. 3*C*) were increased at HU (vs. control) in both groups and increased further in the YOUNG vs. the OLD at RL7 (vs. HU). Thus, a pronounced age effect for a greater effect in the YOUNG was observed at RL7 and in the difference from HU to RL7. $CD163^+DAPI^+$ cells in soleus cross-sections (Fig. 3*D*) were more abundant at HU (vs. control) and were not different by age. $CD68^+CD163^+DAPI^+$ cells in soleus cross-sections (Fig. 3*E*) were greater following HU vs. control. There was a greater density of these cells at RL7 vs. HU in the YOUNG. $CD68^+CD163^-DAPI^+$ cells in gastrocnemius cross-sections (Fig. 3*G*) were relatively rare (2–6 cells/mm^2), but they were higher at RL7 vs. HU in both groups. $CD68^+DAPI^+$ cells in gastrocnemius cross-sections (Fig. 3*I*) were similar in the OLD across all conditions, but the YOUNG showed an increase in this cell population at RL7 vs. HU. There were age-related differences in these cells such that they were lower in the YOUNG vs. OLD at control and RL4. $CD68^-CD163^+DAPI^+$ cells in gastrocnemius cross-sections (Fig. 3*H*) were relatively rare (2–10 cells/mm^2), but they were more abundant in the OLD than in the YOUNG at control and HU. Moreover, the OLD had a lower density of these cells at RL4 and RL7 vs. HU. $CD163^+DAPI^+$ cells in gastrocnemius cross-sections (Fig. 3*J*) were higher in the OLD compared with the YOUNG in the control and HU conditions and a lower density of these cells during RL vs. HU. $CD68^+CD163^+DAPI^+$ cells in gastrocnemius cross-sections (Fig. 3*K*) were higher in the OLD than in the YOUNG at control and at RL4.

To further characterize the anti-inflammatory macrophage phenotype at RL7, we examined soleus and gastrocnemius cross-sections with immunofluorescent costaining of CD163 and CD206, two accepted M2 macrophage markers (Fig. 3*F* and 3*L*). $CD206^+CD163^-DAPI^+$ and $CD206^+DAPI^+$ cells in soleus cross-sections were of greater abundance in YOUNG compared with OLD at RL7. There were no differences in this cell type in the gastrocnemius as a result of experimental condition or age.

Plantaris mRNA expression. Plantaris mRNA expression (Fig. 4) of *Igf-1* was greater at RL4 in both age groups and at RL7 in the YOUNG-only compared with HU. The YOUNG had a higher expression of *Igf-1* throughout RL compared with the OLD. *Ccl2* (C-C motif ligand 2) expression was greater at RL4 in both age groups and at RL7 in the OLD-only compared with HU. In addition, an age difference at RL7 revealed a greater expression in the OLD vs. the YOUNG. *Vegfc* (vascular endothelial growth factor C) and *Irf7* (interferon regulatory factor 7) expressions were less at RL4 in both age groups vs. HU. *Irf7* expression remained reduced at RL7 vs. HU in OLD, and an age effect for the difference between HU and RL7 was seen. Changes in mRNA expression of Cd206 and IL-4 during RL and between age groups did not reach statistical significance.

Gastrocnemius muscle macrophages via flow cytometry. Quantification and characterization of gastrocnemius muscle macrophages via flow cytometry is shown in Fig. 5. $Ly6c^+$ cells were considered proinflammatory monocytes/macro-
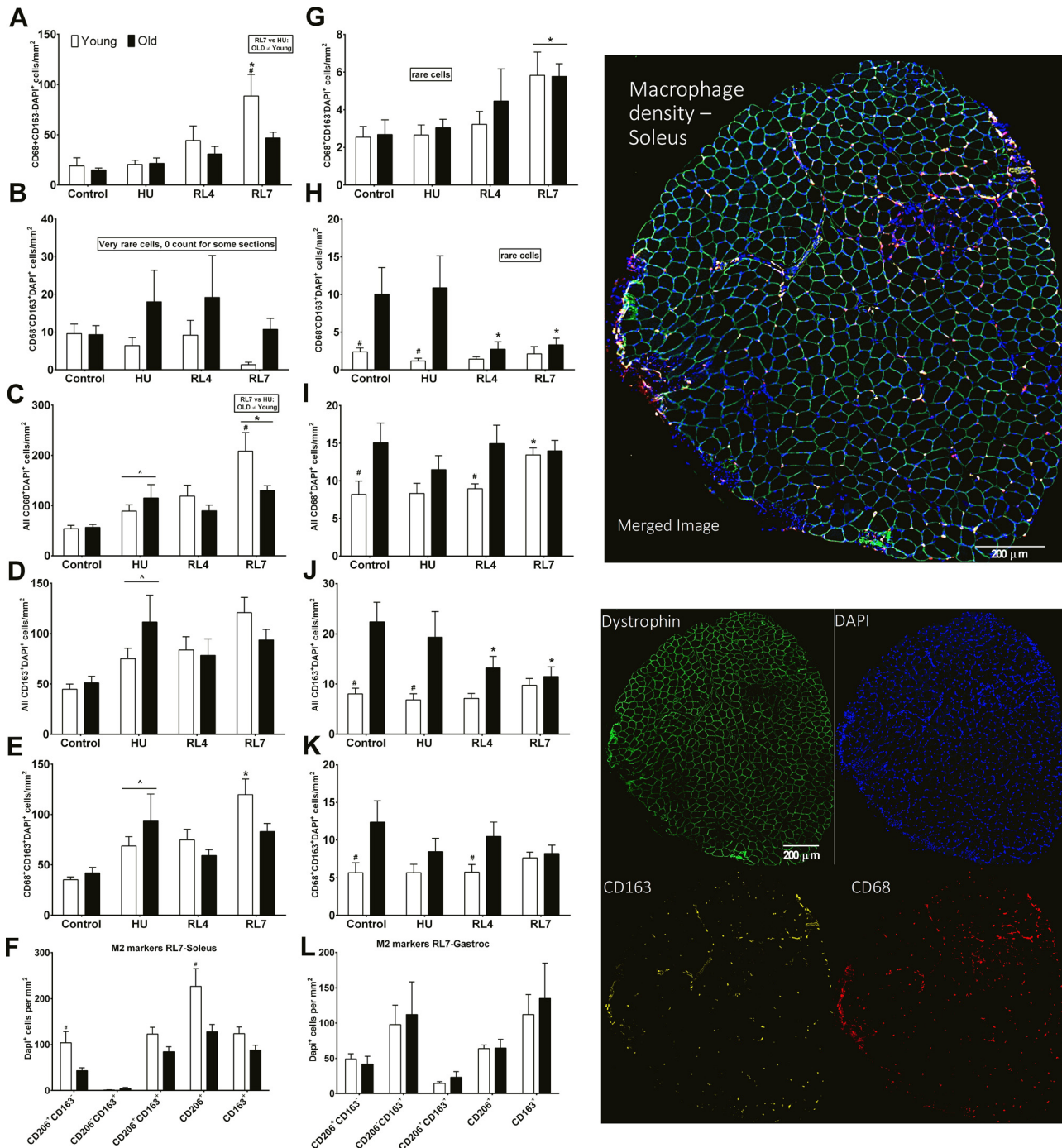
Fig. 3. Immunofluorescence quantification of macrophages in soleus (*A–F*) and gastrocnemius (*G–L*) cross-sections from OLD and YOUNG ambulatory control mice during hindlimb unloading (HU) and reloading (RL) as $CD68^+CD163^-DAPI^+$ (*A, G*), $CD68^-CD163^+DAPI^+$ (*B, H*), All $CD68^+DAPI^+$ (*C, I*), All $CD163^+DAPI^+$ (*D, J*), and $CD68^+CD163^+DAPI^+$ (*E, K*), cells. Further classification of M2-like macrophages as $CD206^-CD163^+DAPI^+$, $CD206^+CD163^-DAPI^+$, All $CD163^+DAPI^+$, All $CD206^+DAPI^+$, and $CD206^+CD163^+DAPI^+$ cells at RL7 (*F, L*). Representative image of CD68, CD163, dystrophin, and DAPI immunofluorescent costaining of a soleus cross-section merged (*M, top right*) and as individual channels (*N, bottom right*). RL4, 4 days of RL; RL7, 7 days of RL. #$P < 0.05$ vs. Old; *$P < 0.05$ vs. HU; ^$P < 0.05$ vs. Control.

phages, and $F4/80^+$ cells were considered resident tissue macrophages (23, 27).

F4/80 cells (percent of CD11b cells; data not shown) were similar across the experimental conditions in the YOUNG. The OLD mice demonstrated a smaller population of these cells at HU (vs. control), which was restored to control levels during RL vs. HU. Thus, an age effect for the difference from control to HU and from HU to RL was observed. When expressed per milligram of muscle (Supplemental Fig. S4) a greater abundance of macrophages was observed at RL4 vs. HU and there were no differences by age.

We classified "M1-like" polarized macrophages as $MHCII^+$-$CD206^-$ and "M2-like" polarized macrophages as $MHCII^-$-$CD206^+$. $MHCII^+CD206^-$ cells (percent $F4/80^+CD11b^+$ cells;
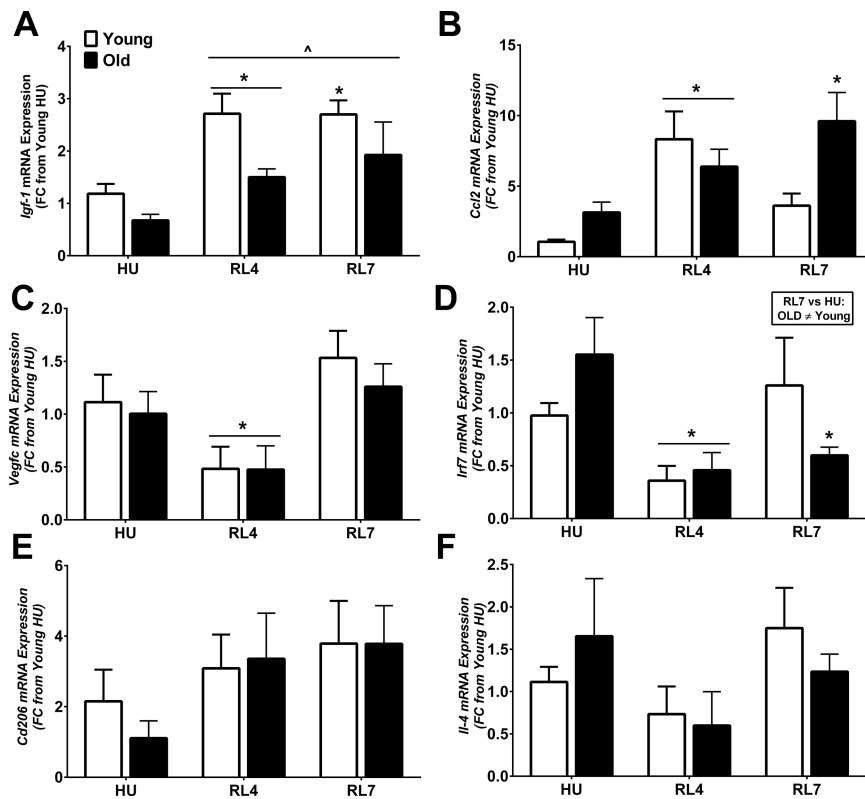
Fig. 4. Plantaris mRNA expression of insulin-like growth factor I (*Igf-1*; *A*), C-C motif ligand 2 (*Ccl2*; *B*), vascular endothelial growth factor C (*Vegfc*; *C*), interferon regulatory factor 7 (*Irf7*; *D*), *Cd206* (*E*), and *Il-4* (*F*) in OLD and YOUNG mice during hindlimb unloading (HU) and reloading (RL). RL4, 4 days of RL; RL7, 7 days of RL; FC, fold change. Expression was normalized to the YOUNG HU group with the geometric mean of *36b4* and *Pparg* as housekeeping genes to examine the effect of age and reloading. $*P < 0.05$ vs. HU; $^P < 0.05$ vs. Control.

Fig. 5*C*) were greater in the YOUNG than in the OLD at control, HU, and RL4. This population of cells in both groups was less following HU compared with control. Although both groups had greater levels of these cells during RL, the YOUNG had the greatest abundance at RL4 (vs. HU) such that an effect of age was evident. MHCII$^+$,CD206$^-$ cells (percent F4/80$^+$CD11b$^+$ cells) per milligram of muscle weight (Supplemental Fig. S4*B*) were higher in the YOUNG vs. the OLD at control and decreased in the YOUNG at HU vs. control. Following RL, both groups demonstrated greater abundance of these cells at RL4 vs. HU.

MHCII$^-$CD206$^+$ cells (percent F4/80$^+$CD11b$^+$ cells; Fig. 5*D*) were higher at HU vs. control and decreased at RL4 vs. HU in both groups. At RL7, the OLD demonstrated a smaller abundance of these cells vs. HU, whereas the YOUNG demonstrated a greater frequency of these cells. MHCII$^-$,CD206$^+$ cells (percent F4/80$^+$CD11b$^+$ cells) per milligram of muscle weight (Supplemental Fig. S4*C*) were similar across experimental conditions and by age.

Next, we examined the ratio of these M2-like to M1-like macrophages (data not shown). A greater ratio was observed at HU vs. control in both groups, yet the OLD increased to a greater extent than the YOUNG. Following RL, the OLD showed a smaller ratio at RL4 and RL7 vs. HU, whereas the YOUNG showed a smaller ratio only at RL4 (vs. HU). The YOUNG also demonstrated a higher ratio of M2 to M1 cells at RL7 (vs. OLD) such that an age effect in the difference from HU to RL7 was evident. The ratio of M2-like to M1-like macrophages per milligram of muscle weight (Supplemental Fig. S4*D*) tended ($P = 0.066$) to be greater in OLD vs. YOUNG at control and HU. The ratio was higher at HU vs. control in both groups. Although both groups showed a decrease in the ratio at RL4 (vs. HU), the YOUNG demonstrated

a lower ratio compared with the OLD. The OLD maintained a lower M2/M1 ratio at RL7 vs. HU, which resulted in an age effect in the difference from HU to RL7 being evident.

Ly6c^{High}F4/80^{High} cells (percent CD11b cells; Fig. 5*E*) were similar by age and at control and HU in both groups. During RL, the YOUNG had fewer Ly6c^{High}F4/80^{High} cells at both RL4 and RL7 (vs. HU) such that an effect of age was present at those time points and in the difference from HU to RL. A similar pattern was seen when cells were normalized to milligrams of muscle weight (Supplemental Fig. S4*E*).

Ly6c^{Low}F4/80^{High} cells (percent CD11b cells; Fig. 5*F*) were similar between control and HU in OLD. During RL, the YOUNG maintained a higher level than the OLD, but no difference from HU to RL was observed in either group. When expressed per milligram of muscle (Supplemental Fig. S4*F*), the YOUNG similarly demonstrated a greater level than the OLD at HU. Following RL, the YOUNG demonstrated a lower abundance at RL4 vs. HU, yet the OLD had a greater abundance at RL4 vs. HU. Thus, an age difference was evident at RL4.

Ly6c^{Medium}F4/80^{Low} cells (percent CD11b cells; Fig. 5*G*) were higher in the OLD after HU and lower in the YOUNG such that a pronounced age effect was observed at HU and in the difference from control to HU. During RL, the YOUNG maintained the level of these cells, whereas the OLD showed a lower abundance (vs. HU). As a result, there was an age effect in the difference from HU to RL (pooled). When expressed per milligram of muscle (Supplemental Fig. S4*G*) the OLD demonstrated a greater abundance at HU vs. control and an age effect was observed at HU and the difference from control to HU. Following RL, these cells were higher in the OLD than in the YOUNG.
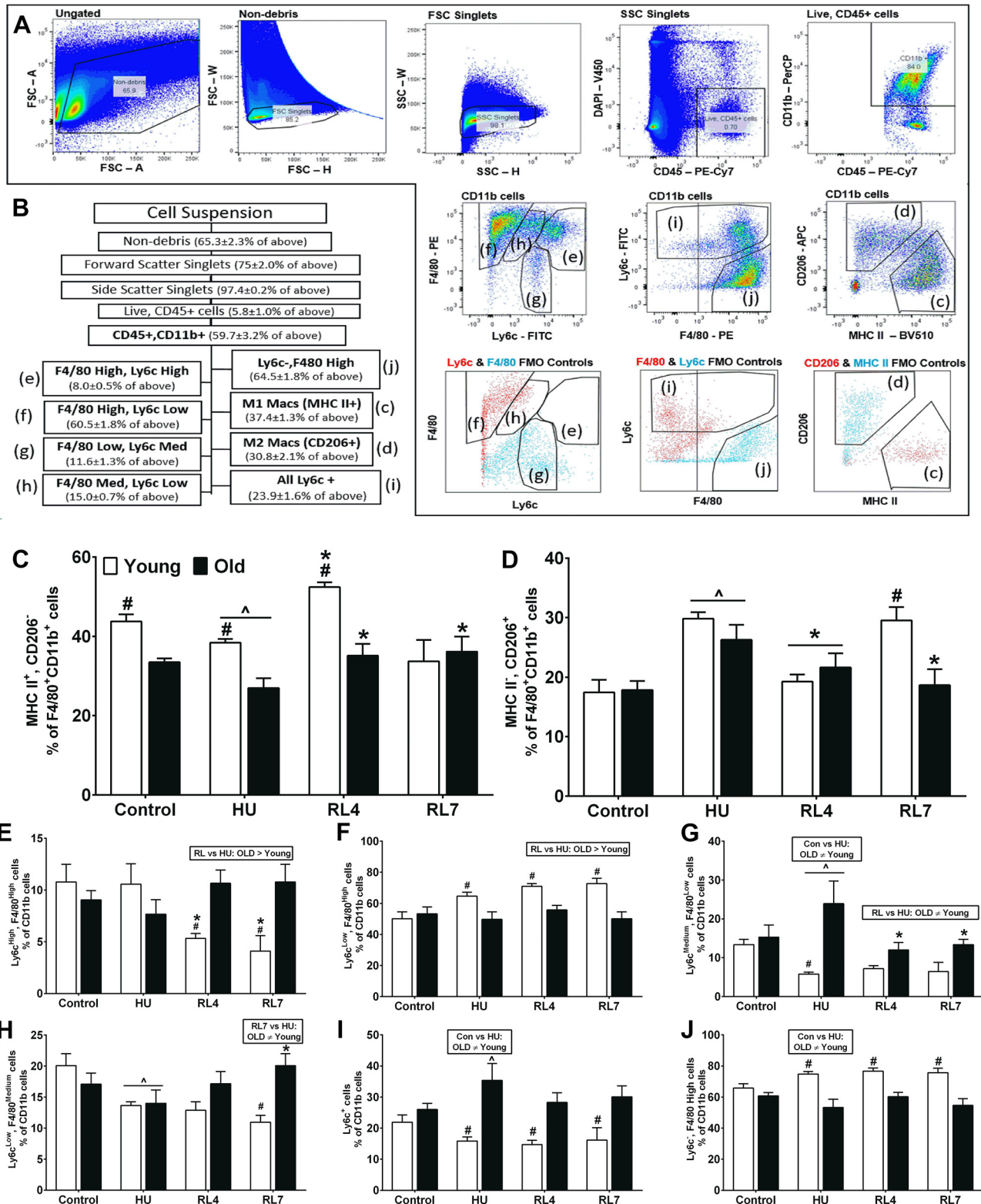
Fig. 5. Immunophenotyping of macrophages in gastrocnemius single-cell suspensions from OLD and YOUNG ambulatory control mice during hindlimb unloading (HU) and reloading (RL). *A*: gating strategy and validation with fluorescence minus-one controls with letters in parentheses denoting populations of interest. After gating out debris, we excluded doublets and selected live (DAPI$^-$)CD45$^+$CD11b$^+$ cells as the myeloid monocyte/macrophage population of interest. *B*: representative quantification of gating strategy, with letters in parentheses denoting populations of interest. Live (DAPI$^-$)CD45$^+$CD11b$^+$ populations of interest (*C, K*). M1-like macrophages (CD11b$^+$F4/80$^+$) as MHC II$^+$CD206$^-$ cells (*C*). M2-like macrophages (CD11b$^+$F4/80$^+$) as MHC II$^-$CD206$^+$ cells (*D*). Ratio of M2-like to M1-like macrophages (F4/80$^+$) (*E*). Ly6c^{High}F4/80^{HIgh} cells (*F*), Ly6c^{Low}F4/80^{HIgh} cells (*G*), Ly6c^{Medium}F4/80^{Low} cells (*H*), Ly6c^{Low}F4/80^{Medium} cells (*I*), Ly6c$^+$F4/80$^-$ cells (*J*), and Ly6c$^-$F4/80$^+$ cells. RL4, 4 days of RL; RL7, 7 days of RL; MHC, myosin heavy chain; FSC, forward scatter; SSC, side scatter. #$P < 0.05$ vs. Old; *$P < 0.05$ vs. HU; ^$P < 0.05$ vs. Control.

Ly6c^{Low}F4/80^{Medium} cells (percent CD11b cells; Fig. 5*H*) were lower at HU compared with control in both groups. Following RL, the OLD displayed a greater abundance vs. the YOUNG, which resulted in a greater abundance in the OLD at RL7 vs. HU. Since the YOUNG were similar at RL vs. HU, an age effect at RL7 and in the difference from HU to RL7 was evident. When expressed per milligram of muscle (Supplemental Fig. S4*H*), differences by age and time were noted only following RL. The OLD demonstrated a greater abundance at RL4 vs. HU; thus, an age effect during RL and in the difference from HU to RL was evident.

Ly6c^{-}F4/80^{High} cells (percent CD11b cells; Fig. 5*I*) were higher in the YOUNG vs. the OLD at HU and following RL (pooled RL vs. HU). An age effect for the difference from control to HU was evident. When expressed per milligram of muscle (Supplemental Fig. S4*I*), the YOUNG had a greater abundance in the control vs. OLD, and the YOUNG showed a smaller abundance of these cells following HU. Following RL, a greater abundance of these cells was observed at RL4 vs. HU.

Ly6c^{+}F4/80^{-} cells (percent CD11b cells; Fig. 5*J*) were greater in the OLD than in the YOUNG at HU and following RL vs. HU. An age effect for the difference from control to HU was evident. When expressed per milligram of muscle (Supplemental Fig. S4*J*), a similar pattern was observed.

Regarding muscle-specific macrophage content, the plantaris (63.1 ± 6.0 cells per mg muscle) had similar macrophage abundance (CD45^{+}CD11b^{+}F4/80^{+} cells) to the gastrocnemius (63.8 ± 7.4 cells per mg muscle), whereas the soleus had greater abundance of macrophages than either plantaris or gastrocnemius (186.8 ± 36.6 cells per mg muscle).

At RL4, we used flow cytometry to examine myeloid cell abundance (per mg muscle) in young and old soleus versus gastrocnemius (Fig. 6). CD45^{+} cells were more abundant in the soleus with no differences by age. CD45^{+}CD11b^{+}, CD45^{+}CD11b^{+}CD64^{+}, CD45^{+}CD11b^{+}CD64^{+}MHCII^{+}CD206^{-}, and CD45^{+}CD11b^{+}CD64^{High}Ly6c^{Low} cells were more abundant in the YOUNG than the OLD in the soleus, and the YOUNG soleus had more of these cells than the YOUNG gastrocemius. CD45^{+}CD11b^{+}CD64^{+}MHCII^{-}CD206^{+} were more abundant in the YOUNG soleus than in the OLD soleus, but overall the gastrocnemius demonstrated higher levels than in the soleus. CD45^{+}CD11b^{+}Ly6c^{+} cells were more abundant in the soleus than in the gastrocnemius and were greater in the OLD than in the YOUNG gastrocnemius. Finally, CD45^{+}CD11b^{+}CD64^{Low}Ly6c^{+} were more abundant in the soleus than in the gastrocnemius and were greater in OLD than in YOUNG in both muscles.

Gastrocnemius and soleus CD11b^{+} cell mRNA expression. Gene expression of *Cd206* and *Vegfc* was lower, while Retnla was higher in OLD vs. YOUNG in gastrocnemius *Cd11b^{+}* cells at RL4 (Fig. 7*A*), and there was no difference by age at RL7 (Fig. 7*B*). In the soleus, at RL4, mRNA expression of *Cd206*, *Il-4*, and *Vegfc* was lower, whereas *Retnla* and *Il-10* were higher in OLD vs. YOUNG (Fig. 7*C*). When mRNA expression was compared in gastrocnemius resident *Cd11b* cells from RL4 to RL7 by age (Fig. 7*D*), *Il-1β*, *Il-6*, *tumor necrosis factor-α*, *Infγ*, and *Cd206* were lower in RL7 vs. RL4, whereas *Il-4*, *Vegfc*, *Retnla*, and *Irf7* were higher in RL7 vs. RL4. With this normalization, the OLD had lower *Cd206* mRNA expression at RL4 and less *Retnla* expression at RL7. When mRNA expression in gastrocnemius versus soleus resident *Cd11b* cells at RL4 were compared by age (Fig. 7*E*), *Il-6*, *Infγ*, and *Vegfc* were lower in in the soleus. The OLD soleus has less Il-4 expression than the YOUNG soleus muscle, while also demonstrating greater expression of *Retnla*, *Tbfβ*, and *Il-10* than expression levels in both YOUNG soleus and OLD gastrocnemius. With this normalization, the OLD had lower *Cd206* mRNA expression in the gastrocnemius, whereas *Vegfc* expression was suppressed in both muscles with aging.

DISCUSSION

In the context of muscle regrowth following disuse, we used flow cytometry and cell sorting to characterize the skeletal muscle monocyte/macrophage polarization and activation patterns in male mice. These experiments revealed dynamic skeletal muscle macrophages in young mice similar to the panoply of literature using immunofluorescence or immunohistochemistry on muscle cross-sections. With our use of this gold standard method to quantify immune cells, we demonstrated, for the first time, that older (~25 mo) mice have an altered skeletal muscle monocyte/macrophage characterization and muscle-specific abundance in the week following recovery from disuse (hindlimb unloading) that is concurrent with impaired muscle regrowth compared with young mice. These are important findings specific to physiological muscle disuse and subsequent regrowth in aging and distinct from the supraphysiological damage/injury and subsequent regeneration more commonly studied in skeletal muscle immunology.

The field of skeletal muscle immunology has made inroads toward dissecting skeletal muscle pathology regeneration responses (9, 10, 48). In addition, research from the laboratory of Dr. James Tidball (48), among others, has demonstrated well
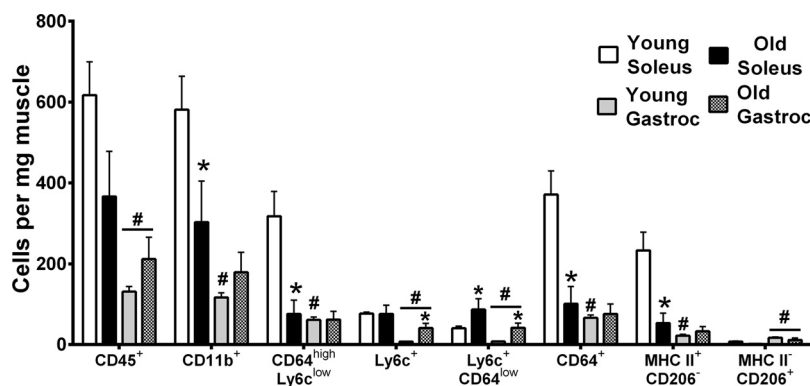

Fig. 6. Monocyte/macrophage cell abundance (per mg muscle) at 4 days of reloading (RL4) in OLD and YOUNG soleus and gastrocnemius (Gastroc) muscle single-cell suspensions. After gating out debris, doublets were excluded and selected, live (DAPI^{-})CD45^{+} cells as the myeloid populations of interest. CD64^{+}, Ly6c^{+}, CD64^{high}Ly6c^{low}, and CD64^{low}Ly6c^{+} cells were from the CD45^{+}CD11b^{+} population and MHC II^{+}CD206^{-} and MHCII^{-}CD206^{+} cells were from the CD64^{+} population. MHC, myosin heavy chain. #$P < 0.05$ vs. soleus; *$P < 0.05$ vs. YOUNG for that muscle group.
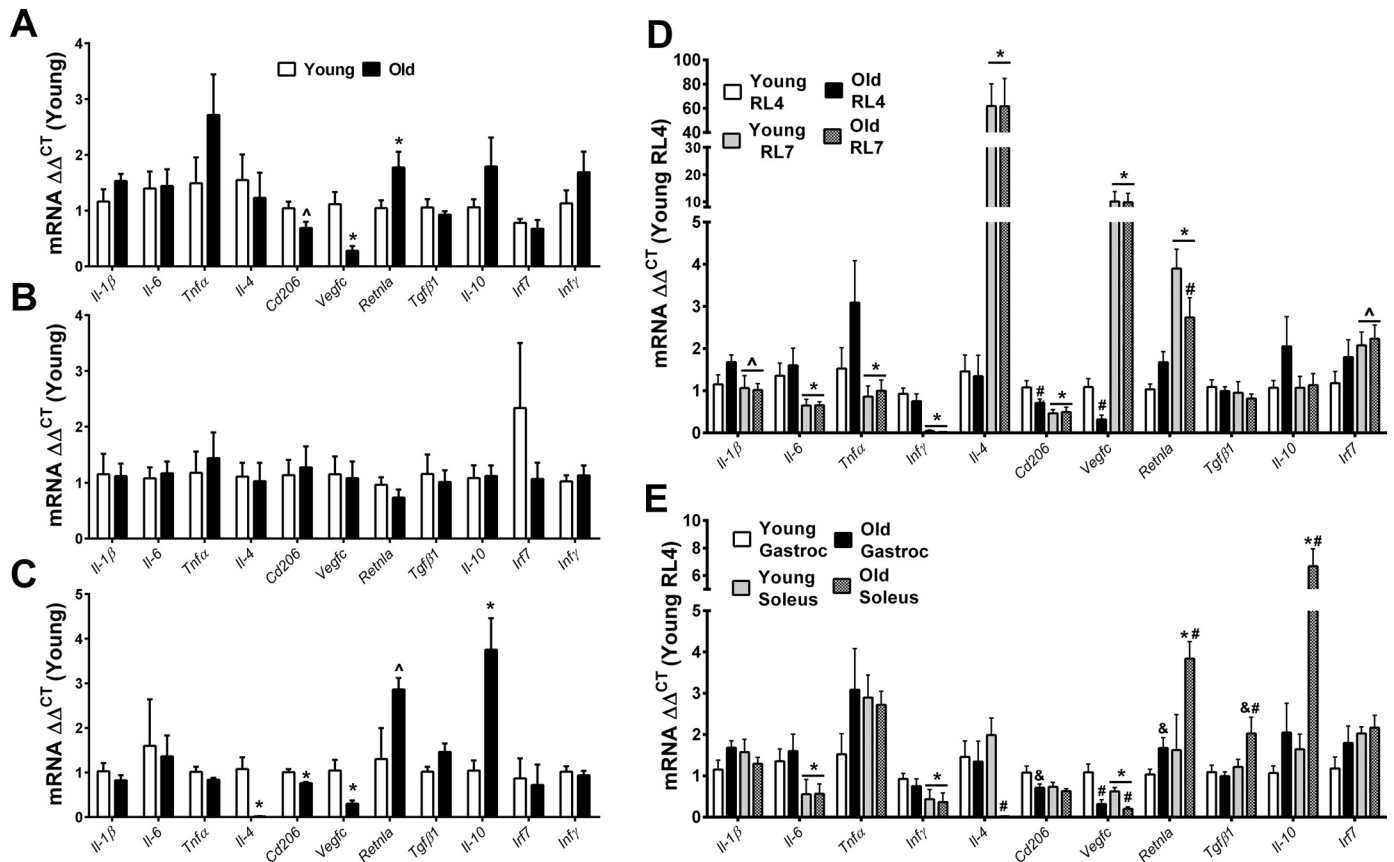
Fig. 7. mRNA expression of live (DAPI⁻) CD45⁺CD11b⁺ cells in OLD and YOUNG mice by age at 4 days of reloading (RL4) gastrocnemius (*A*), 7 days of RL (RL7) gastrocnemius (*B*), and at RL4 soleus (*C*). *D*: comparing mRNA expression in gastrocnemius resident CD11b cells from RL4 to RL7 by age. *E*: comparing mRNA expression in gastrocnemius vs. soleus resident CD11b cells at RL4 by age. *$P < 0.05$, ^$P = 0.056$ vs. YOUNG (*A–C*); *$P < 0.05$, ^$P < 0.08$ vs. RL4 (*D*); #$P < 0.05$ vs. YOUNG for that time point (*D*); *$P < 0.05$ vs. gastrocnemius for that age (*E*); #$P < 0.05$, &$P < 0.08$ vs. YOUNG for that muscle group (*F*). IL, interleukin; TNFα, tumor necrosis factor-α; VEGFc, vascular endothelial growth factor C; TGFβ, transforming growth factor-β; IRF7, interferon regulatory factor 7; INFγ, interferon-γ.

the skeletal muscle macrophage responses from disuse and specifically muscle regrowth following disuse, but only in young rodents (12, 14, 18, 19, 43, 46–49). Their work in this minimal-injury model (hindlimb unloading followed by reambulation/reloading) demonstrates a classical increase in proinflammatory (M1-like) macrophages that precedes an increase in anti-inflammatory (M2-like) macrophages in the first week of ambulatory recovery following disuse (46, 48). In addition, several reports using loss (monocyte/macrophage deletion) of gain- (immunotherapy) of-function experiments demonstrate a requirement of macrophages for complete and rapid regrowth (12, 14, 35, 49). The sparse level of muscle damage (26) and central nucleation with this model (26, 48) suggests that muscle macrophages are contributing much more than the more common supporting role toward the activation and proliferation of satellite cells in muscle regeneration (9, 10). This and the evidence that knockdown of paired box 7-expressing satellite cells does not impair muscle regrowth (26) suggests that macrophages exert other beneficial functions [i.e., release of cytokines and growth factors like Igf-I and macrophage colony-stimulating factor (M-CSF)] to promote rapid muscle regrowth (9). Similar to these previous reports in young rats, we also demonstrate a relative increase in M1-like macrophages (CD11b⁺F4/80⁺MHC II⁺CD206⁻) early (at RL4) that is re-

solved and replaced by an M2-like macrophage (CD11b⁺F4/80⁺MHC II⁻CD206⁺) response later (at RL7).

It is well documented that aging is accompanied by impaired muscle regrowth following disuse atrophy (24, 25, 44, 53). It was unknown whether this impaired regrowth was due, in part, to skeletal muscle macrophages, which are clearly important to maximize regrowth in young animals. Only one study thus far has examined a single macrophage marker using immunofluorescence at one late recovery time point (14 days recovery) following disuse in aging animals, thereby missing valuable earlier time points and polarization information during the recovery process (53). Interestingly, the older mice in our experiments do not show the aforementioned macrophage plasticity of young rats, and this impairment is contemporaneous with the impaired regrowth of aging muscle we demonstrate in the gastrocnemius and soleus muscles. In addition, the older mice demonstrated an accumulation of cells with the proinflammatory marker Ly6c, which likely reflects an abundance of inflammatory monocytes. Intriguingly, in the gastrocnemius, monocyte expansion starts during disuse and carries foward into the RL phase, suggesting that disuse itself may have an influence on skeletal muscle monocyte/macrophage activity (12, 19, 34, 47), which we speculate may further "overactivate" the initial skeletal muscle immune response and

contribute to impaired muscle regrowth. The fact that disuse precedes the modest RL stress of HU is likely why these age-related responses are distinct from the effects of aging on muscle macrophages due to the much more damaging eccentric exercise (40). Yet, old mice clearly demonstrate impaired skeletal muscle recovery from ischemia-reperfusion and other toxin injury models (1, 3, 7) that may be mediated, in part, by impaired macrophage function. Indeed, aging in general impairs macrophage polarization (30), and macrophages in aging skeletal muscle are dysregulated during regeneration from toxin injury (36). We now demonstrate, for the first time, a similar phenomenon during the regrowth of aged skeletal muscle following disuse.

The accumulation of inflammatory monocytes ($Ly6c^+$ cells) in the gastrocnemius and soleus combined with elevated plantaris *Ccl2* mRNA expression in aged mice during recovery suggests that these immune cells from old mice do not have a dysregulated recruitment and migration of monocytes. We acknowledge that plantaris mRNA expression is limited in its ability to characterize immune cell responses found in the other muscles studied herein, but there are some interesting patterns in this muscle that deserve brief discussion. As suggested in a previous report (42), we demonstrate impaired *Igf-I* expression within aged muscle following recovery from disuse. Also, the old have greater *Ccl2* expresasion during recovery than the young, which corresponded to less *Irf7* expression. Since *Irf7* is a lymphoid-specific marker essential for monocytes to differentiate from macrophages (29) these data could indicate that the old muscles are continually recuiting monocytes during recovery, but, unlike young muscle, their ability to convert them to macrophages may be impaired; thus, recruitment of these inflammatory monocytes is prolonged in aged muscle.

To further explore the phenotype of the monocytes/macrophages, we sorted $CD45^+CD11b^+$ cells from the gastrocnemius and soleus during recovery. When young versus old were compared at specific time points we found no difference at RL7 in the gastrocnemius but rather a divergent M2-like mRNA expression pattern in the old early in recovery (4 days RL) in both soleus and gastrocnemius, suggesting an altered activation status of the tissue resident macrophages. Regardless of these differences, both age groups demonstrated an mRNA expression pattern that reflected a shift from the M1-like to the M2-like phenotype from RL4 to RL7 in the gastrocnemius. Intriguingly, the mRNA expression pattern examining the muscle-specific and age-dependent effects early in recovery (RL4) suggested a differential activation pattern between muscles and a premature M2-like response in the old soleus. Thus, rather than an impairment in monocyte/macrophage recruitment to the gastrocnemius, it is more likely that these aged mice possess an ineffective immunomodulation of recruited and resident cells.

Another interesting finding was that in the gastrocnemius the old may have a reduced percentage and concentration of M1-like resident tissue macrophages compared with the young. The reasons for this are unknown, but it may explain why aging skeletal muscle is characterized by a greater abundance and stiffness of extracellular matrix (54), since this macrophage phenotype may promote collagen turnover (52).

We were able to expand the use of flow cytometry to the soleus during muscle recovery. In general, we observed greater concentrations of myeloid cells in the old soleus during early recovery (RL4). Also, the old soleus had fewer resident tissue macrophages (high CD64 expression and low Ly6c expression) with a M1-like phenotype ($MHC\ II^+CD206^-$) compared with the young. This pattern in the old soleus somewhat resembled what we found in the old gastrocnemius and is likely reflective of the slower rate of regrowth in these muscles. Although the gastrocnemius did not display a difference in myeloid, monocyte or resident tissue cells between old and young, the old gastrocnemius hosted a greater level of infiltrating inflammatory monocytes and macrophages ($CD11b^+Ly6c^+$ and $CD11b^+Ly6c^+CD64^{Low}$ cells). Similarly, the old soleus contained a greater abundance (vs. young) of these infiltrating cells which we speculate may indicate a reduced capacity with aging to differentiate the infiltrating monocytes and macrophages into the resident tissue macrophages ($CD64^+$). Overall, these data comparing the age-related myeloid cell response in the soleus versus the gastrocnemius during early recovery may suggest that there is an impairment in monocyte/macrophage recruitment and activation in the soleus with aging.

The literature concerning rodent skeletal muscle immune cells during RL following disuse has been exclusively dominated by the use of semiquantitative immunohistochemistry or immunofluorescence analysis in (12, 18, 19, 43, 46–49) and limited to experiments in young animals. Although flow cytometry has been used on muscle single-cell suspensions to immunophenotype in response to supraphysiological injury, this method has not yet been applied to the physiologically relevant disuse/regrowth model. As such, a strength of this investigation is the novel use of flow cytometry to validate 20 or more years of immune cell data generated in young animals and to take this application a step further by characterizing the disuse/regrowth response in aging animals. Quantification and characterization of macrophages conducted through the use of immunohistochemistry/immunofluorescence on skeletal muscle cross-sections is only semiquanitative, imprecise, and potentially inaccurate, especially when larger muscles are considered, as we demonstrate here with differences in macrophage quantification in the gastrocnemius with immunofluorescence and flow cytometry. Our immunofluoresence quantification of macrophages on soleus cross-sections demonstrated increased macrophage density with RL and is in line with reports in the literature and the general pattern of greater resistent muscle macrophages in young vs. old mice at RL7. However, our immunofluorescence quantification of macrophages on gastrocnemius cross-sections was not consistent with the immunophenotyping we conducted via flow cytometry on single cell suspensions in the same muscle. This does well to highlight the challenge of utilizing a single 8-μm slice of large and complex muscle to quantify muscle macrophages. The soleus muscle is likley more uniform across its length and thus immunohistochemistry or immunofluoresence quantification of macrophages cross-sections from that muscle are probably more representative of the muscle as a whole as opposed to the gastrocnemius, where one slice runs the risk of a less acurate representation of the data. Another challenge to immune cell identification via immunohistochemistry or immunofluoresence is that these methods are restricted in the number of antigens (<3 or 4) and have limited quantitative application and potential for nonspecificity of the macrophage marker antigens. Macrophage markers commonly utilized in these methods may nonspecifically bind to neutrophils, dendritic

cells, satellite cells, or other cell types (37, 48). To overcome these limitations, we utilized the novel application of flow cytometry on gastrocnemius single-cell suspensions to specifically identify and quantify muscle macrophages through a precise and specific myeloid-gating strategy (Fig. 5). Utilizing these methods, we revealed divergent presence of macrophage and monocyte phenyotypes in skeletal muscle of aged vs. young mice following muscle disuse and recovery.

An unexpected finding of this study was that in control conditions soleus macrophage abundance (with immunofluoresence and flow cytometry) was higher than the more fast-twitch plantaris and gastrocnemius which shared macrophage similar abundance. We also demonstrated greater macrophage abundance (in young muscle) in the soleus compared with the gastrocnemius at RL4. The underlying explanations for these differences in macrophage abundance between these muscles are not entirely known (28) but are likely reflective of the muscle composition, activity level, or level of damage upon releading and warrants further examination.

Finally, our characterization of M1-like and M2-like macrophages is an oversimplification. Although many authors make these generalizations regarding macrophages, the reality is that macrophages exist on a spectrum (32), particularly in vivo, where macrophages will express markers for both phenotypes concurrently. In this study, we demonstrate a similar pattern with macrophages expressing both markers, but we classify as M1- or M2-like when those cells demonstrate a predominance of a specific M1 or M2 marker. Also, there is a possibility, that the $Ly6C^{High}$ population that we classify as inflammatory monocytes/macrophages could include inflammatory neutrophils. We would consider this highly unlikely, since elevation of neutrophils in skeletal muscle following recovery from disuse has been seen only within 2 days of RL (19, 43, 47) but likely resolves shortly after (4 and 7 days) as in our current study, since RL from disuse induces very little muscle damage, unlike cardiotoxin injury (51). However, accumulation of these cells is delayed in aging skeletal muscle (40), and the possibility of prolonged neutrophil accumulation in aged skeletal muscle during recovery from disuse warrants further investigation. Last, macrophage activation would be better characterized by experiments using protein quantification via ELISA or immunostaining of these immune cells.

Our data are mostly descriptive, and future focused experiments (such as adoptive transfer of old and young immune cells) are needed to specifically test whether this impairment is centered around the aged immune cells, aged myofibers, or some interaction effect. Strategies to provide skeletal muscle-activated macrophages via timely intramuscular injection of M1 (39) or M2 (23) polarized macrophages demonstrated improved muscle repair and regrowth following injury. In addition, activation of recruited and resident muscle immune cells via timely intramuscular injection of M-CSF demonstrated improved muscle regrowth following disuse (15). Thus, it is probable that similar strategies hold promise to improve muscle regrowth in aged skeletal muscle following disuse.

Characterization of the aging skeletal muscle immune response in this minimal-injury model (disuse/regrowth) is invaluable because of the frequency of such insidious inactivity and recovery events during the aging process. A large proportion of these older adults will take months to years to fully recover their muscle function, with many never regaining pre-hospitalization levels (5, 6, 11, 20–22). Over a lifetime, it is reasonable to expect repeated cycles of hospitalizations and incomplete muscle recovery, further accelerating muscle and functional decline in this vulnerable population (16). Thus, there exists a need for a strong understanding of cellular and molecular events that govern muscle regrowth in older adults following disuse in order to develop appropriate mechanistic-based interventions to offset these deficits in muscle and strength.

DISCLOSURES

No conflicts of interest, financial or otherwise, are declared by the authors.

AUTHOR CONTRIBUTIONS

P.T.R. and M.J.D. conceived and designed research; P.T.R., A.I.M., Z.S.M., J.J.P., D.B.N., C.C.L., J.E.G., and V.R.M. performed experiments; P.T.R., A.I.M., C.C.L., and G.J.S. analyzed data; P.T.R., A.C.K., T.B.H., G.K., R.M.O., and M.J.D. interpreted results of experiments; P.T.R. prepared figures; P.T.R. and M.J.D. drafted manuscript; P.T.R., A.I.M., and M.J.D. edited and revised manuscript; P.T.R., A.I.M., Z.S.M., J.J.P., D.B.N., C.C.L., J.E.G., V.R.M., A.C.K., T.B.H., G.J.S., G.K., R.M.O., and M.J.D. approved final version of manuscript.

REFERENCES

1. **Arnold L, Henry A, Poron F, Baba-Amer Y, van Rooijen N, Plonquet A, Gherardi RK, Chazaud B.** Inflammatory monocytes recruited after skeletal muscle injury switch into antiinflammatory macrophages to support myogenesis. *J Exp Med* 204: 1057–1069, 2007. doi:10.1084/jem.20070075.

2. **Baehr LM, West DW, Marcotte G, Marshall AG, De Sousa LG, Baar K, Bodine SC.** Age-related deficits in skeletal muscle recovery following disuse are associated with neuromuscular junction instability and ER stress, not impaired protein synthesis. *Aging (Albany NY)* 8: 127–146, 2016. doi:10.18632/aging.100879.

3. **Blau HM, Cosgrove BD, Ho AT.** The central role of muscle stem cells in regenerative failure with aging. *Nat Med* 21: 854–862, 2015. doi:10.1038/nm.3918.

5. **Boyd CM, Landefeld CS, Counsell SR, Palmer RM, Fortinsky RH, Kresevic D, Burant C, Covinsky KE.** Recovery of activities of daily living in older adults after hospitalization for acute medical illness. *J Am Geriatr Soc* 56: 2171–2179, 2008. doi:10.1111/j.1532-5415.2008.02023.x.

6. **Boyd CM, Ricks M, Fried LP, Guralnik JM, Xue QL, Xia J, Bandeen-Roche K.** Functional decline and recovery of activities of daily living in hospitalized, disabled older women: the Women's Health and Aging Study I. *J Am Geriatr Soc* 57: 1757–1766, 2009. doi:10.1111/j.1532-5415.2009.02455.x.

7. **Brack AS, Muñoz-Cánoves P.** The ins and outs of muscle stem cell aging. *Skelet Muscle* 6: 1, 2016. doi:10.1186/s13395-016-0072-z.

9. **Chazaud B.** Macrophages: supportive cells for tissue repair and regeneration. *Immunobiology* 219: 172–178, 2014. doi:10.1016/j.imbio.2013.09.001.

10. **Chazaud B, Brigitte M, Yacoub-Youssef H, Arnold L, Gherardi R, Sonnet C, Lafuste P, Chretien F.** Dual and beneficial roles of macrophages during skeletal muscle regeneration. *Exerc Sport Sci Rev* 37: 18–22, 2009. doi:10.1097/JES.0b013e318190ebdb.

11. **Covinsky KE, Palmer RM, Fortinsky RH, Counsell SR, Stewart AL, Kresevic D, Burant CJ, Landefeld CS.** Loss of independence in activities of daily living in older adults hospitalized with medical illnesses: increased vulnerability with age. *J Am Geriatr Soc* 51: 451–458, 2003. doi:10.1046/j.1532-5415.2003.51152.x.

12. **Deng B, Wehling-Henricks M, Villalta SA, Wang Y, Tidball JG.** IL-10 triggers changes in macrophage phenotype that promote muscle growth and regeneration. *J Immunol* 189: 3669–3680, 2012. doi:10.4049/jimmunol.1103180.

13. **Drummond MJ, Addison O, Brunker L, Hopkins PN, McClain DA, LaStayo PC, Marcus RL.** Downregulation of E3 ubiquitin ligases and mitophagy-related genes in skeletal muscle of physically inactive, frail older women: a cross-sectional comparison. *J Gerontol A Biol Sci Med Sci* 69: 1040–1048, 2014. doi:10.1093/gerona/glu004.

14. **Dumont N, Frenette J.** Macrophages protect against muscle atrophy and promote muscle recovery in vivo and in vitro: a mechanism partly dependent on the insulin-like growth factor-1 signaling molecule. *Am J Pathol* 176: 2228–2235, 2010. doi:10.2353/ajpath.2010.090884.

15. **Dumont NA, Frenette J.** Macrophage colony-stimulating factor-induced macrophage differentiation promotes regrowth in atrophied skeletal muscles and C2C12 myotubes. *Am J Pathol* 182: 505–515, 2013. doi:10.1016/j.ajpath.2012.10.010.

16. **English KL, Paddon-Jones D.** Protecting muscle mass and function in older adults during bed rest. *Curr Opin Clin Nutr Metab Care* 13: 34–39, 2010. doi:10.1097/MCO.0b013e328333aa66.

17. **Ferreira JA, Crissey JM, Brown M.** An alternant method to the traditional NASA hindlimb unloading model in mice. *J Vis Exp* 10: 2467, 2011. doi:10.3791/2467.

18. **Frenette J, Cai B, Tidball JG.** Complement activation promotes muscle inflammation during modified muscle use. *Am J Pathol* 156: 2103–2110, 2000. doi:10.1016/S0002-9440(10)65081-X.

19. **Frenette J, St-Pierre M, Côté CH, Mylona E, Pizza FX.** Muscle impairment occurs rapidly and precedes inflammatory cell accumulation after mechanical loading. *Am J Physiol Regul Integr Comp Physiol* 282: R351–R357, 2002. doi:10.1152/ajpregu.00189.2001.

20. **Gill TM, Allore H, Guo Z.** The deleterious effects of bed rest among community-living older persons. *J Gerontol A Biol Sci Med Sci* 59: M755–M761, 2004. doi:10.1093/gerona/59.7.M755.

21. **Gill TM, Allore HG, Holford TR, Guo Z.** Hospitalization, restricted activity, and the development of disability among older persons. *JAMA* 292: 2115–2124, 2004. doi:10.1001/jama.292.17.2115.

22. **Gill TM, Gahbauer EA, Han L, Allore HG.** The relationship between intervening hospitalizations and transitions between frailty states. *J Gerontol A Biol Sci Med Sci* 66A: 1238–1243, 2011. doi:10.1093/gerona/glr142.

23. **Hammers DW, Rybalko V, Merscham-Banda M, Hsieh P-L, Suggs LJ, Farrar RP.** Anti-inflammatory macrophages improve skeletal muscle recovery from ischemia-reperfusion. *J Appl Physiol (1985)* 118: 1067–1074, 2015. doi:10.1152/japplphysiol.00313.2014.

24. **Hébuterne X, Schneider S, Peroux JL, Rampal P.** Effects of refeeding by cyclic enteral nutrition on body composition: comparative study of elderly and younger patients. *Clin Nutr* 16: 283–289, 1997. doi:10.1016/S0261-5614(97)80013-1.

25. **Hvid L, Aagaard P, Justesen L, Bayer ML, Andersen JL, Ørtenblad N, Kjaer M, Suetta C.** Effects of aging on muscle mechanical function and muscle fiber morphology during short-term immobilization and subsequent retraining. *J Appl Physiol (1985)* 109: 1628–1634, 2010. doi:10.1152/japplphysiol.00637.2010.

26. **Jackson JR, Mula J, Kirby TJ, Fry CS, Lee JD, Ubele MF, Campbell KS, McCarthy JJ, Peterson CA, Dupont-Versteegden EE.** Satellite cell depletion does not inhibit adult skeletal muscle regrowth following unloading-induced atrophy. *Am J Physiol Cell Physiol* 303: C854–C861, 2012. doi:10.1152/ajpcell.00207.2012.

27. **Kohno S, Yamashita Y, Abe T, Hirasaka K, Oarada M, Ohno A, Teshima-Kondo S, Higashibata A, Choi I, Mills EM, Okumura Y, Terao J, Nikawa T.** Unloading stress disturbs muscle regeneration through perturbed recruitment and function of macrophages. *J Appl Physiol (1985)* 112: 1773–1782, 2012. doi:10.1152/japplphysiol.00103.2012.

28. **Krause MP, Al-Sajee D, D'Souza DM, Rebalka IA, Moradi J, Riddell MC, Hawke TJ.** Impaired macrophage and satellite cell infiltration occurs in a muscle-specific fashion following injury in diabetic skeletal muscle. *PLoS One* 8: e70971, 2013. doi:10.1371/journal.pone.0070971.

29. **Lu R, Pitha PM.** Monocyte differentiation to macrophage requires interferon regulatory factor 7. *J Biol Chem* 276: 45491–45496, 2001. doi:10.1074/jbc.C100421200.

30. **Mahbub S, Deburghgraeve CR, Kovacs EJ.** Advanced age impairs macrophage polarization. *J Interferon Cytokine Res* 32: 18–26, 2012. doi:10.1089/jir.2011.0058.

31. **McKenzie AI, Briggs RA, Barrows KM, Nelson DS, Kwon OS, Hopkins PN, Higgins TF, Marcus RL, Drummond MJ.** A pilot study examining the impact of exercise training on skeletal muscle genes related to the TLR signaling pathway in older adults following hip fracture. *J Appl Physiol (1985)* 122: 68–75, 2017. doi:10.1152/japplphysiol.00714.2016.

32. **Mosser DM, Edwards JP.** Exploring the full spectrum of macrophage activation. *Nat Rev Immunol* 8: 958–969, 2008. [Erratum in: *Nat Rev Immunol* 10: 460, 2010.] doi:10.1038/nri2448.

33. **Murphy MM, Keefe AC, Lawson JA, Flygare SD, Yandell M, Kardon G.** Transiently active Wnt/β-catenin signaling is not required but must be silenced for stem cell function during muscle regeneration. *Stem Cell Reports* 3: 475–488, 2014. doi:10.1016/j.stemcr.2014.06.019.

34. **Kawanishi N, Funakoshi T, Machida S.** Time-course study of macrophage infiltration and inflammation in cast immobilization-induced atrophied muscle of mice. *Muscle Nerve* 57: 1006–1013, 2018. doi:10.1002/mus.26061.

35. **Ohira T, Wang XD, Ito T, Kawano F, Goto K, Izawa T, Ohno H, Kizaki T, Ohira Y.** Macrophage deficiency in osteopetrotic (*op/op*) mice inhibits activation of satellite cells and prevents hypertrophy in single soleus fibers. *Am J Physiol Cell Physiol* 308: C848–C855, 2015. doi:10.1152/ajpcell.00348.2014.

36. **Patsalos A, Simandi Z, Hays TT, Peloquin M, Hajian M, Restrepo I, Coen PM, Russell AJ, Nagy L.** In vivo GDF3 administration abrogates aging related muscle regeneration delay following acute sterile injury. *Aging Cell* 17: e12815, 2018. doi:10.1111/acel.12815.

37. **Paulsen G, Egner I, Raastad T, Reinholt F, Owe S, Lauritzen F, Brorson S-H, Koskinen S.** Inflammatory markers CD11b, CD16, CD66b, CD68, myeloperoxidase and neutrophil elastase in eccentric exercised human skeletal muscles. *Histochem Cell Biol* 139: 691–715, 2013. doi:10.1007/s00418-012-1061-x.

38. **Reidy PT, Lindsay CC, McKenzie AI, Fry CS, Supiano MA, Marcus RL, LaStayo PC, Drummond MJ.** Aging-related effects of bed rest followed by eccentric exercise rehabilitation on skeletal muscle macrophages and insulin sensitivity. *Exp Gerontol* 107: 37–49, 2018. doi:10.1016/j.exger.2017.07.001.

39. **Rybalko V, Hsieh P-L, Merscham-Banda M, Suggs LJ, Farrar RP.** The development of macrophage-mediated cell therapy to improve skeletal muscle function after injury. *PLoS One* 10: e0145550, 2015. doi:10.1371/journal.pone.0145550.

40. **Sloboda DD, Brown LA, Brooks SV.** Myeloid cell responses to contraction-induced injury differ in muscles of young and old mice. *J Gerontol A Biol Sci Med Sci* 73: 1581–1590, 2018. doi:10.1093/gerona/gly086.

41. **Smith LR, Barton ER.** SMASH—semi-automatic muscle analysis using segmentation of histology: a MATLAB application. *Skelet Muscle* 4: 21, 2014. doi:10.1186/2044-5040-4-21.

42. **Spangenburg EE, Abraha T, Childs TE, Pattison JS, Booth FW.** Skeletal muscle IGF-binding protein-3 and -5 expressions are age, muscle, and load dependent. *Am J Physiol Endocrinol Metab* 284: E340–E350, 2003. doi:10.1152/ajpendo.00253.2002.

43. **St Pierre BA, Tidball JG.** Differential response of macrophage subpopulations to soleus muscle reloading after rat hindlimb suspension. *J Appl Physiol (1985)* 77: 290–297, 1994. doi:10.1152/jappl.1994.77.1.290.

44. **Suetta C, Hvid LG, Justesen L, Christensen U, Neergaard K, Simonsen L, Ortenblad N, Magnusson SP, Kjaer M, Aagaard P.** Effects of aging on human skeletal muscle after immobilization and retraining. *J Appl Physiol (1985)* 107: 1172–1180, 2009. doi:10.1152/japplphysiol.00290.2009.

45. **Tanner RE, Brunker LB, Agergaard J, Barrows KM, Briggs RA, Kwon OS, Young LM, Hopkins PN, Volpi E, Marcus RL, LaStayo PC, Drummond MJ.** Age-related differences in lean mass, protein synthesis and skeletal muscle markers of proteolysis after bed rest and exercise rehabilitation. *J Physiol* 593: 4259–4273, 2015. doi:10.1113/JP270699.

46. **Tidball JG.** Interactions between muscle and the immune system during modified musculoskeletal loading. *Clin Orthop Relat Res* 403, *Suppl*: S100–S109, 2002. doi:10.1097/00003086-200210001-00012.

47. **Tidball JG, Berchenko E, Frenette J.** Macrophage invasion does not contribute to muscle membrane injury during inflammation. *J Leukoc Biol* 65: 492–498, 1999. doi:10.1002/jlb.65.4.492.

48. **Tidball JG, Villalta SA.** Regulatory interactions between muscle and the immune system during muscle regeneration. *Am J Physiol Regul Integr Comp Physiol* 298: R1173–R1187, 2010. doi:10.1152/ajpregu.00735.2009.

49. **Tidball JG, Wehling-Henricks M.** Macrophages promote muscle membrane repair and muscle fibre growth and regeneration during modified muscle loading in mice in vivo. *J Physiol* 578: 327–336, 2007. doi:10.1113/jphysiol.2006.118265.

50. **Varga T, Mounier R, Horvath A, Cuvellier S, Dumont F, Poliska S, Ardjoune H, Juban G, Nagy L, Chazaud B.** Highly dynamic transcriptional signature of distinct macrophage subsets during sterile inflammation, resolution, and tissue repair. *J Immunol* 196: 4771–4782, 2016. doi:10.4049/jimmunol.1502490.

51. **Wang H, Melton DW, Porter L, Sarwar ZU, McManus LM, Shireman PK.** Altered macrophage phenotype transition impairs skeletal muscle regeneration. *Am J Pathol* 184: 1167–1184, 2014. doi:10.1016/j.ajpath.2013.12.020.

52. **Wang Y, Wehling-Henricks M, Samengo G, Tidball JG.** Increases of M2a macrophages and fibrosis in aging muscle are influenced by bone marrow aging and negatively regulated by muscle-derived nitric oxide. *Aging Cell* 14: 678–688, 2015. doi:10.1111/acel.12350.

53. **White JR, Confides AL, Moore-Reed S, Hoch JM, Dupont-Versteegden EE.** Regrowth after skeletal muscle atrophy is impaired in aged rats, despite similar responses in signaling pathways. *Exp Gerontol* 64: 17–32, 2015. doi:10.1016/j.exger.2015.02.007.

54. **Wood LK, Kayupov E, Gumucio JP, Mendias CL, Claflin DR, Brooks SV.** Intrinsic stiffness of extracellular matrix increases with age in skeletal muscles of mice. *J Appl Physiol (1985)* 117: 363–369, 2014. doi:10.1152/japplphysiol.00256.2014.

55. **Zhang X, Trevino MB, Wang M, Gardell SJ, Ayala JE, Han X, Kelly DP, Goodpaster BH, Vega RB, Coen PM.** Impaired mitochondrial energetics characterize poor early recovery of muscle mass following hind limb unloading in old mice. *J Gerontol A Biol Sci Med Sci* 73: 1313–1322, 2018. doi:10.1093/gerona/gly051.